HELDA
HELSINGIN YLIOPISTO
HELSINGFORS UNIVERSITET
UNIVERSITY OF HELSINKI

UNIVERSITY OF HELSINKI

https://helda.helsinki.fi

First direct kinetic measurement of i -C4H5 (CH2CHCCH2) + O-2 reaction : Toward quantitative understanding of aromatic ring formation chemistry

Eskola, Arkke J.

2021

Eskola , A J , Reijonen , T T , Pekkanen , T T , Heinonen , P , Joshi , S P & Timonen , R S 2021 , ' First direct kinetic measurement of i -C4H5 (CH2CHCCH2) + O-2 reaction : Toward quantitative understanding of aromatic ring formation chemistry ' , Proceedings of the Combustion Institute , vol. 38 , no. 1 , pp. 813-821 . https://doi.org/10.1016/j.proci.2020.06.031

http://hdl.handle.net/10138/347107
https://doi.org/10.1016/j.proci.2020.06.031

cc_by_nc_nd
acceptedVersion

Downloaded from Helda, University of Helsinki institutional repository.

This is an electronic reprint of the original article.

This reprint may differ from the original in pagination and typographic detail.

Please cite the original version.

First Direct Kinetic Measurement of *i*-C_4H_5 (CH_2CHCCH_2) + O_2 Reaction: Toward Quantitative Understanding of Aromatic Ring Formation Chemistry

Arkke J. Eskola, Timo T. Reijonen, Timo T. Pekkanen, Petri Heinonen, Satya P. Joshi, Raimo S. Timonen*

Molecular Science, Department of Chemistry, University of Helsinki, FI-00560 Helsinki, Finland

*Corresponding author's contact information:

Department of Chemistry, PO BOX 55 (A.I. Virtasen aukio 1), FIN-00014 University of Helsinki, Finland

Phone: +358 50 4489288

email: arkke.eskola@helsinki.fi

Colloquium: 1. Gas-Phase Reaction Kinetics

Supplemental Material is available.

Total length of the paper prepared using MS Word (6200 max): 5905

Word equivalent length of main text: 3823; equations: 25; nomenclature: 0; references: 595; Scheme 1. 55; Fig 1. 334; Fig 2. 365; Fig 3. 383; Fig 4. 165; Fig 5. 160

We do not intend to pay color charges.

Abstract

The kinetics of the *i*-C_4H_5 (buta-1,3-dien-2-yl) radical reaction with molecular oxygen has been measured over a wide temperature range (275 – 852 K) at low pressures (0.8 – 3 Torr) in direct, time-resolved experiments. The measurements were performed using a laminar flow reactor coupled to photoionization mass spectrometer (PIMS), and laser photolysis of either chloroprene (2-chlorobuta-1,3-diene) or isoprene was used to produce the resonantly stabilized *i*-C_4H_5 radical. Under the experimental conditions, the measured bimolecular rate coefficient of *i*-C_4H_5 + O_2 reaction is independent of bath gas density and exhibits weak, negative temperature dependency, and can be described by the expression $k_3 = (1.45 \pm 0.05) \times 10^{-12} \times (T/298\ \mathrm{K})^{-(0.13 \pm 0.05)}$ $\mathrm{cm^3\ s^{-1}}$. The measured bimolecular rate coefficient is surprisingly fast for a resonantly stabilized radical. Under combustion conditions, the reactions of *i*-C_4H_5 radical with ethylene and acetylene are believed to play an important role in forming the first aromatic ring. However, the current measurements show that *i*-C_4H_5 + O_2 reaction is significantly faster under combustion conditions than previous estimations suggest and, consequently, inhibits the soot forming propensity of *i*-C_4H_5 radicals. The bimolecular rate coefficient estimates used for the *i*-C_4H_5 + O_2 reaction in recent combustion simulations show significant variation and are up to two orders of magnitude slower than the current, measured value. All estimates, in contrast to our measurements, predict a positive temperature dependency. The observed products for the *i*-C_4H_5 + O_2 reaction were formaldehyde and ketene. This is in agreement with the one theoretical study available for *i*-C_4H_5 + O_2 reaction, which predicts the main bimolecular product channels to be $H_2CO + C_2H_3 + CO$ and $H_2CCO + CH_2CHO$.

KEYWORDS: Radical reaction kinetics, photoionization mass spectrometer, *i*-C_4H_5 radical, oxidation, soot formation

1. Introduction

Polycyclic aromatic hydrocarbons (PAHs) are formed in incomplete combustion of hydrocarbon fuels and are likely precursors of soot particles. Internal combustion engine generated PAHs and soot have several adverse effects, for example on human health, and consequently there is significant interest to mitigate or even prevent their formation. To reach this goal, predictive physico-chemical models for soot formation are needed, which require reliable rate coefficients for key elementary reactions that promote or inhibit aromatic ring and PAH formation. However, the rate coefficients of many elementary reactions potentially important in aromatic ring and PAHs formation are unknown and the rate coefficients often have to be estimated, because high-quality experimental and/or theoretical values are rarely available.

The primary focus in understanding PAH and soot formation chemistry is often on the formation of "the first aromatic ring" from small aliphatic constituents, which is expected to be the kinetic bottleneck in the reaction sequence leading to PAHs.[1] Although there are different views on the main reactions and mechanism(s) leading to the formation of the first aromatic ring and its subsequent growth to larger PAHs[1-3], it has been generally accepted that resonantly-stabilized radicals (RSRs) play a major role in these processes.[4] Radical – radical recombination reactions of resonantly-stabilized propargyl,

$$C_3H_3 + C_3H_3 \rightarrow \text{benzene / fulvene / phenyl} + H \quad (1)$$

and allyl (C_3H_5) radicals are probably the most important reactions leading to aromatic ring formation in odd-carbon pathways. The even-carbon pathway

$$i\text{-}C_4H_5 + C_2H_2 \rightarrow \text{fulvene} + H \quad (2)$$

to benzene *via* fulvene has been shown to be especially important in 1,3-butadiene flames[3, 5] and has also been shown to play an important role in other flames.[6] The chemical structures of benzene, fulvene, and phenyl radical are shown in Scheme S1.

Oxidation reactions of RSRs compete with the aromatic ring forming reactions (reactions (1) and (2), for example) and thus inhibit soot formation. Propargyl[7] and substituted propargyl (e.g. CH_3CCCH_2)[8] radicals are RSRs and react only slowly with O_2 at temperatures 1000 – 1500 K and have bimolecular rate coefficients in the range ~ 2 – 5 × 10^{-14} cm^3 s^{-1}, whereas non-RSRs vinyl[9] and methyl-vinyl[10, 11] radicals react much faster with O_2 in the above temperature range with bimolecular rate coefficients close to ~ 1 × 10^{-11} cm^3 s^{-1}; difference in the reactivity of vinyl and propargyl radicals is more than a factor of 200. Allyl, 1-methylallyl, and 2-methylallyl are also RSRs and are probably even less reactive toward O_2 than propargylic radicals.[12-15] All this make it interesting to investigate and measure the kinetics of the

$$i\text{-}C_4H_5 + O_2 \rightarrow \text{Products} \qquad (3)$$

reaction, because i-C_4H_5 is a RSR that has vinylic and allenic resonance structures as shown in Scheme 1. Consequently, one might expect reaction (3) to be similarly slow as the above discussed propargyl- or allyl-type radical + O_2 reactions. On the other hand, i-C_4H_5 can also be thought of as an α-vinyl-substituted vinyl radical and, therefore, exhibit similar reactivity toward O_2 as vinylic radicals. However, heat of formation calculations at the G4 level of theory show that the allenic structure is about 8 kcal mol^{-1} lower in energy than the vinylic configuration and thus the allenic structure is predicted to be the dominant configuration.[16]

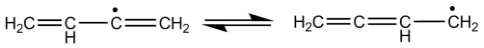

Scheme 1. Two resonance (Kekulé) structures of i-C_4H_5 radical.
Left: vinylic structure, Right: allenic structure.

In addition to the rate of disappearance of i-C_4H_5 radical due to the reaction with O_2, also the identity of the reaction products play important role in any chemical mechanism to model PAHs and soot formation. Mechanisms, which have been used recently to model benzene formation under flame temperatures[5] (T ~ 1500 K) and lower flame temperatures[17] ($T \leq$ 1200 K), assume that the only important channel of reaction (3) is i-C_4H_5 + O_2 → H_2CCO + CH_2CHO. However, as one can observe from the enthalpy profile of i-C_4H_5 + O_2 reaction shown in Figure 1, other reactions channels may also be important. The enthalpy profile is adapted from the work of Rutz et al.[18], where the energies are

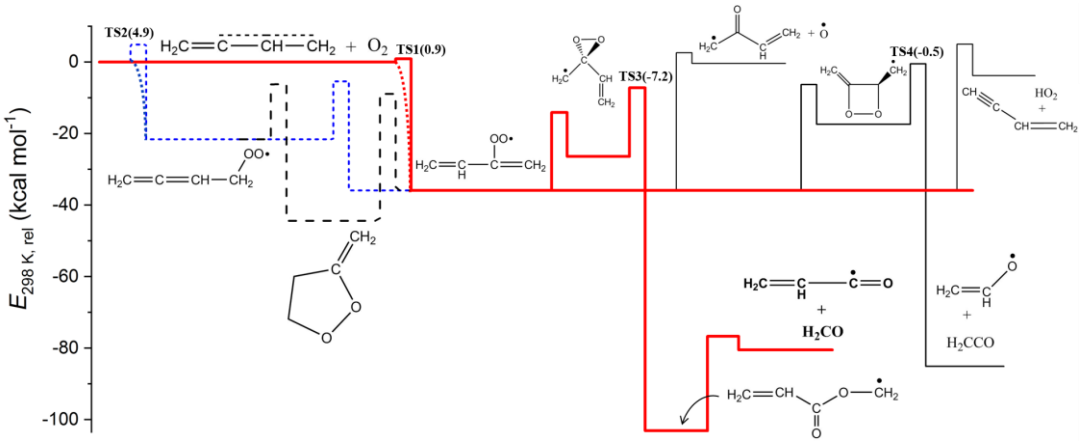

Figure 1. Enthalpy profile of i-C_4H_5 + O_2 reaction according to Rutz[18] *et al. with G3SX enthalpies. See text on discussion of transition-state 1(**TS1**) and **TS2** energies.*

computed at the G3SX level of theory. Especially the highly exothermic reaction channel leading to H_2CO + CH_2CHCO, followed by prompt, chemically-activated decomposition of CH_2CHCO to C_2H_3 + CO, may play an important role, not least because the highest energy transition state of the channel is more than 7 kcal/mol below the energy of the reactants (see Figure 1). To our knowledge, the current work shows the first kinetic measurements of the *i*-C_4H_5 radical and reaction (3).

2. Experimental

Excimer laser photolysis was used for radical production and photoionization mass-spectrometry (PIMS) was utilized for time-resolved detection of radical decay and product formation profiles. The experimental apparatus has been described in detail in a previous publication.[19] The experiments were performed in tubular flow reactor and the flowing gas mixture consisted of the radical precursor (chloroprene or isoprene), O_2 in varying amounts (< 1 %), and helium bath gas in large excess. The plug flow rate of the gas mixture through the temperature-controlled reactor was about 4 – 5 m s^{-1}, which ensured that the gas mixture was completely replaced between laser pulses when a repetition rate of 5 Hz was used. In the experiments a 17 mm inner diameter quartz tube coated with boric oxide (B_2O_3)[20] was employed over the experimental temperature range. The reactor was heated using PID-controlled resistive heating and a temperature uniformity of about ± 5 K was obtained below 600 K. At higher temperatures, the temperature uncertainty was somewhat larger, about ± 10 K. Oxygen flows were measured using the pressure-rise-in-a-known-volume –method (no mass-flow-controller was

used in the current work) and the photolytic precursor was supplied into the reactor using a temperature-controlled bubbler.

The *i*-C_4H_5 radical (CH_2CHCCH_2) was produced homogenously either from chloroprene ($CH_2CHCClCH_2$) or isoprene ($CH_2CHC(CH_3)CH_2$) precursor by excimer laser (Coherent COMPexPro 201) photolysis at 248 nm along the flow reactor. Two different precursors were used to show that the results do not depend on the identity of the radical precursor. Already in the first measurements of the *i*-C_4H_5 + O_2 reaction it became apparent that *i*-C_4H_5 was not the only radical that appeared at *m/z* = 53. This observation can be explained by examining the energetics of chloroprene photolysis at 248 nm shown in Figure S1. Importantly, Figure S1 shows that in addition to the *i*-C_4H_5 radical, also the 3-methylpropargyl radical can and almost certainly is formed when chloroprene is photolyzed at 248 nm. Similarly important is that *n*-C_4H_5 formation, based on the MN15/Def2TZPV energies, is energetically inaccessible. All other products potentially formed appear at *m/z* ratios different from 53. A list of observed products from chloroprene photolysis at 248 nm, the main source of *i*-C_4H_5 radical in this work, is provided in the Supplemental Material. For chloroprene / isoprene photolysis we can write:

$$CH_2CHC(Cl/CH_3)CH_2 + h\nu(248\ nm) \rightarrow CH_2CHCCH_2 + Cl/CH_3 \quad (P1)$$

$$\rightarrow CH_2CCCH_3 + Cl/CH_3 \quad (P2)$$

$$\rightarrow \text{Other products} \quad (P3)$$

One might initially think that the formation of two different RSRs at the same *m/z* ratio would preclude any kinetic measurement of the *i*-C_4H_5 + O_2 reaction. Fortunately, CH_2CCCH_3 (3-methylpropargyl) radical reacts more than an order of magnitude slower with O_2 than *i*-C_4H_5, enabling separation of their reaction rates in time-resolved experiments. Note that we have very recently performed direct kinetic measurements of the 3-methylpropargyl + O_2 reaction over a wide temperature range, enabling us to interpret and process current measurements correctly.[8] The adiabatic ionization energies (*AIE*) of *i*-C_4H_5 and 3-methylpropargyl radicals have been measured to be *AIE*(*i*-C_4H_5) = 7.60 ± 0.05 eV[21] and *AIE*(3-methylpropargyl) = 7.93 ± 0.01 eV[22], respectively, showing these *AIE*s are close to each

other. In this work a microwave-powered resonance lamp was employed to photoionize CH_2CHCCH_2 and CH_2CCCH_3 radicals with a combination of a CaF_2 salt window and a Cl_2 gas lamp to produce radiation in the range 8.9 – 9.1 eV. That is, both *i*-C_4H_5 and 3-methylpropargyl radicals were ionized.

The ions were mass-selected using a quadrupole mass-spectrometer based on their *m/z* ratio prior to their detection by an off-axis electron multiplier. The temporal ion count signal (see insets in Figure 2) was amplified, discriminated, and recorded using a multichannel scaler from 20 ms before and up to 70 ms after each laser pulse and transferred to a computer for further analysis. Typically a decay signal profile was accumulated from 7000 to 15000 repetitions to obtain adequate signal-to-noise ratio before the subsequent analysis.

Experiments were performed under pseudo-first-order conditions ($[CH_2CHCCH_2] + [CH_2CCCH_3] \ll [O_2]$) with low initial radical concentrations. Under these circumstances, the following reactions contributed to the decay rate at $m/z = 53$.

$$CH_2CHCCH_2 + O_2 \rightarrow \text{products} \quad (3)$$

$$CH_2CCCH_3 + O_2 \rightarrow \text{products} \quad (4)$$

$$CH_2CHCCH_2 \xrightarrow{k_{3wall}} \text{heterogeneous loss} \quad (3W)$$

$$CH_2CCCH_3 \xrightarrow{k_{4wall}} \text{heterogeneous loss} \quad (4W)$$

Since two radicals, CH_2CHCCH_2 and CH_2CCCH_3, with the same (exact) mass are produced in the photolysis of chloroprene (isoprene) and subsequently react with O_2 and on reactor wall, a double-exponential function $[R] = A \times exp(-k_3't) + B \times exp(-k_4't)$ was fitted to the pre-photolysis-signal-subtracted data by the non-linear least-squares method. Here [R] is a signal proportional to the sum of $[CH_2CHCCH_2]$ and $[CH_2CCCH_3]$ at time *t* and the fitted parameters k_3' and k_4' are the pseudo-first-order decay rate coefficients of CH_2CHCCH_2 and CH_2CCCH_3 radicals, respectively, and A and B are the corresponding signal intensities. The value for k_{4wall} was obtained by plotting the obtained k_4'

values as function of [O_2] and then performing a linear fit, with the intercept of the fit giving k_{4wall}. Note that the employed oxygen concentrations were such a low that the values obtained for k_4' were close to k_{4wall}, especially in the high temperature measurements. The wall rate of the *i*-C_4H_5 radical, k_{3wall}, was subsequently obtained by fitting the above double-exponential function to the decay rate signal of m/z = 53 measured without added O_2 and fixing the second exponent with the k_{4wall} as determined above. The wall-rate determination was done in this fashion, because the double-exponential function could not be reliably fitted to the wall rate signal unless one of the exponents was fixed. Since the only significant reactions consuming radical CH_2CHCCH_2 during the experiments were reactions 3 and 3W, the bimolecular reaction rate coefficient $k_3(CH_2CHCCH_2 + O_2)$ could be obtained from the slope of the k_3' versus [O_2] plot according to the equation $k_3' = k_3(CH_2CHCCH_2 + O_2) \times [O_2] + k_{3wall}$. A typical bimolecular plot to obtain $k_3(CH_2CHCCH_2 + O_2)$ is shown in Figure 2, see chapter 3.1 for details.

The main photolytic precursor, chloroprene (2-chloro-1,3-butadiene), was synthetized by a modified literature procedure[23] from 3,4-dichloro-1-butene. See the Supplemental Material for details. The purity of the chloroprene precursor used in the experiments was better than 97 %. Especially, 1-chloro-1,3-butadiene content, which could result in *n*-C_4H_5 (buta-1,3-dien-1-yl) radical production, was less than 1%. Both chloroprene and isoprene (Sigma-Aldrich, > 99% purity) samples were degassed by several freeze−pump−thaw cycles before use.

3. Results and discussion

3.1 Kinetics and products of the i-C_4H_5 + O_2 reaction

The results of the bimolecular rate coefficient measurements of reaction (3) are presented in Table S1 along with the corresponding experimental conditions. The estimated overall uncertainty of the bimolecular reaction rate coefficient measurements is ± 30%. An example plot of first order decay rate coefficients k_3' and k_4' plotted *versus* [O_2] at T = 852 K are shown in Figure 2. The ion signal profile at m/z = 53 shown in the upper inset of Figure 2 originates from both CH_2CHCCH_2 and CH_2CCCH_3

radicals; the faster portion of the decay originates from the *i*-C_4H_5 + O_2 reaction and the slower portion is mainly due to the wall reaction of 3-methylpropargyl. Because reaction (3) is over 100 times faster than reaction (4)[8] under the experimental conditions, the decay rates of these reactions can be reliably separated.

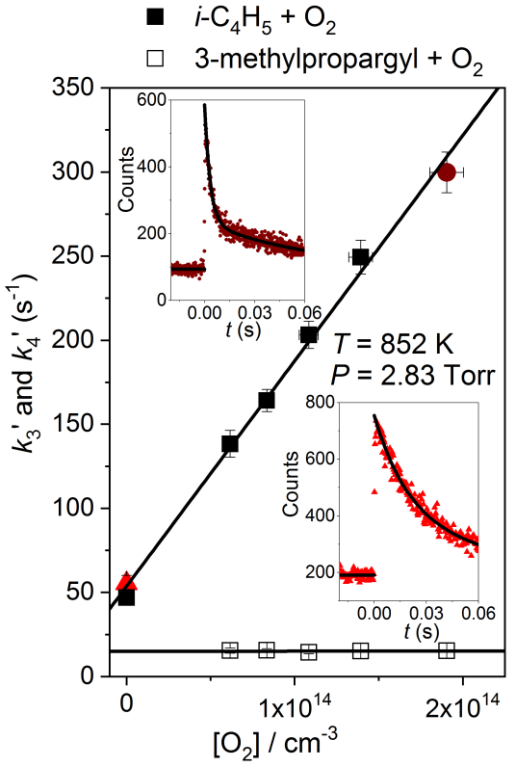

Figure 2. Plot of the first order i-C_4H_5 and 3-methylpropargyl decay rate coefficients k_3' and k_4' versus $[O_2]$ at T = 852 K and 2.83 Torr pressure (see table S1). Insets show actual ion signal profiles for the combined i-C_4H_5 and 3-methylpropargyl decays in the absence of the O_2-reactant (right) and in the presence of the $[O_2] = 1.9 \times 10^{14}$ cm^{-3} (left). Values of k_{3wall}' shown as solid black square and solid red triangle at $[O_2] = 0$ in the plot were measured at first and the end of experiments and k_{4wall}' in the fits was fixed to the value obtained from extrapolating k_4' values to $[O_2] = 0$. Uncertainties are one-standard deviation (1σ).

Experiments were also performed to find reaction products for reaction (3). Photolysis of chloroprene at 248 nm was the sole *i*-C_4H_5 radical source in the experiments to search reaction products. These measurements were performed at room temperature, because reaction (4) or any propargyl- or allyl-type radical reaction with O_2 at room temperature is essentially an addition reaction to form a peroxyl radical and no bimolecular products are formed.[8, 12] A small amount of propargyl radicals is formed in the photolysis of chloroprene at 248 nm, but vinyl and 1-chlorovinyl radicals are not formed (see Supplemental Material). The observed products of reaction (3) are ketene (H_2CCO) and formaldehyde (H_2CO), whose formation rates at 304 K and 2.03 Torr agree with the decay rate of *i*-C_4H_5 within 2σ

fitting uncertainty (see Figure 3). Based on the work of Rutz et al.[18], ketene and formaldehyde are produced by different reaction channels (see Figure 1). The product channel that produces formaldehyde also produces CH_2CHCO, but this product was not observed in our experiments. Szpunar et al. have derived from their experimental results an upper limit of 23 ± 3 kcal/mol for the zero-point-corrected barrier for the $CH_2CHCO \rightarrow C_2H_3 + CO$ unimolecular dissociation reaction.[24] It can be seen from Figure 1 that chemically-activated $CH_2CHCO + H_2CO$ products are formed with

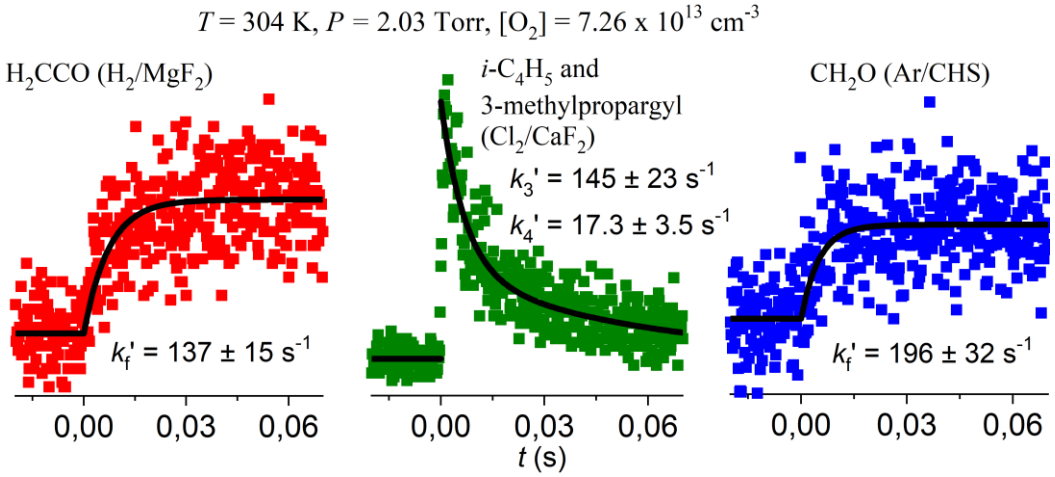

Figure 3. Plots of i-C_4H_5 and 3-methylpropargyl radical decay with fit results (k_3' and k_4') and observed formations and fits of ketene and formaldehyde as products of i-C_4H_5 + O_2 reaction. Chloroprene was photolytic precursor and uncertainties shown are one-standard deviation (1σ). Ketene and formaldehyde formation kinetics agree within 2σ-uncertainty with i-C_4H_5 decay rate.

more than 70 kcal/mol excess energy shared between them. While it is difficult to know exactly how the excess energy is distributed between the two fragments, it is probable that CH_2CHCO radical is formed with enough excess energy to undergo chemically-activated decomposition to $C_2H_3 + CO$, which would explain why no CH_2CHCO was observed. Note that any C_2H_3 radical formed would produce additional formaldehyde by the fast $C_2H_3 + O_2 \rightarrow H_2CO + HCO$ reaction. That is, potentially a significant portion of the H_2CO signal shown in Figure 3 originates from this reaction.

The other product of the ketene producing channel is vinoxy radical, CH_2CHO (see Figure 1). This channel is also highly exothermic, with ketene and vinoxy radical formed with about 80 kcal/mol of excess energy shared between them. Miller et al.[25] have measured that at an internal energy of 41 ± 2 kcal/mol or more, the chemically-activated vinoxy radical first isomerizes to acetyl radical (CH_3CO) and then dissociates to form $CH_3 + CO$. This high threshold energy might reduce importance of any significant chemically-activated vinoxy radical decomposition, in which case the $CH_2CHO + O_2$

reaction is the most likely main sink of vinoxy radicals. The bimolecular rate coefficient of the $CH_2CHO + O_2$ reaction at 300 K and around 1–2 Torr pressure is 1×10^{-13} cm^3s^{-1}, which is an order of magnitude smaller than the rate coefficient observed for reaction (3).[26] In addition, the main product of this reaction under these conditions is the formation of a peroxyl radical, whereas the OH + CO + H_2CO product channel has a yield of only 20 %.[26] Therefore, it is unlikely that the observed formaldehyde originates from the $CH_2CHO + O_2$ reaction. Consequently, it is concluded that formaldehyde and ketene are the primary products of reaction (3) and originate from different reaction channels, in agreement with the computations of Ruiz et al. (see Figure 1).

Figure 4 shows the results of the direct kinetic measurements of *i*-$C_4H_5 + O_2$ reaction *versus* temperature. No pressure dependency was observed for reaction (3). Also shown in Figure 4 is an unweighted fit to the experimental data, which returned the following pressure-independent expression:

$$k_3(i\text{-}C_4H_5 + O_2) = (1.45 \pm 0.05) \times 10^{-12} \times (T/298\ \mathrm{K})^{-(0.13 \pm 0.05)}\ \mathrm{cm^3\ s^{-1}} \qquad \text{(F1)}$$

The uncertainties shown are 1σ. A few measurements were performed using isoprene as the photolytic precursor and these measurements are in good agreement with the chloroprene measurements–a strong indication that the decay signals have been correctly interpreted and the reaction of interest has been successfully isolated. The 95 % confidence limits in Figure 4 show that negative temperature dependency is indeed highly likely for this reaction. Figure S2 compares the bimolecular rate coefficients of *i*-$C_4H_5 + O_2$ and $CH_2CCCH_3 + O_2$ reactions as a function of temperature and illustrates the large difference (≥ 100×) in their reactivity.

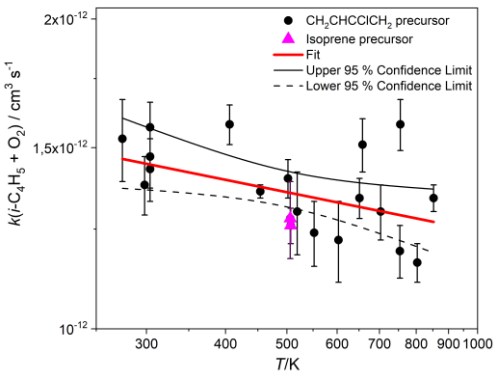

Figure 4. Plot of bimolecular rate coefficients of i-C_4H_5 + O_2 reaction measured in this work versus temperature. Also shown are the obtained fit to the data and 95 % confidence limits.

It is certainly interesting that the *i*-C_4H_5 + O_2 reaction, in contrast to reactions of similar-sized propargylic and allylic RSRs with O_2, is relatively fast, shows weak negative temperature dependency, and is independent of pressure even at low temperatures. Current results strongly suggest that at least one of the two possible O_2 addition channels (see Figure 1) is barrierless. If both addition channels had a barrier, one would expect the rate coefficient of reaction (3) to be several orders of magnitude slower at room temperature and exhibit positive temperature dependency. This observation is in disagreement with the computational work of Rutz et al..[18] There is already quite a large body of evidence for alkyl + O_2 and alkenyl + O_2 radical reactions, both experimental and computational, which consistently shows that these reactions are barrierless. For example, (1) *n*-C_4H_9 + O_2 and *s*-C_4H_9 + O_2,[27] (2) RSR allyl C_3H_5 + O_2 and RSR substituted allyl $CH_2CHCHCH_2CH_3$ + O_2,[12, 28] (3) and vinyl C_2H_3 + O_2 and substituted vinyl CH_3CCH_2 + O_2 and CH_3CHCH + O_2 radical reactions[11, 19] do not show any sign of having a reaction barrier above the energy of the reactants. Multi-reference methods are typically needed to locate the variational transition state for the initial radical + O_2 addition reaction. Particularly for RSR + O_2 reactions single-reference methods are likely to find an addition barrier, but when multi-reference effects are properly accounted for, the barrier is expected to vanish.[28, 29]

The *i*-C_4H_5 + O_2 bimolecular rate coefficient is only about a factor of five slower than the vinyl + O_2 rate coefficient at room temperature and two and a half times faster than the high-pressure allyl + O_2 rate coefficient.[9, 12] In many respects, reaction (3) is more similar to the O_2 reactions of vinylic radicals than to RSR + O_2 reactions. The observed pressure independence and weak, almost negligible negative temperature dependency of reaction (3) bimolecular rate coefficient possess close similarity to the behavior of vinyl and substituted vinyl radicals in reactions with O_2 at $T \geq 300$ K.[9, 11] High-fidelity calculations of vinyl + O_2 and methyl-vinyl + O_2 reactions[9, 10] show that capture-rate coefficient, corresponding to k_∞, agree precisely with the bimolecular rate coefficients obtained from low-pressure experiments performed over wide temperature ranges.[11, 19, 30] The similar behavior

between vinyl + O_2 and *i*-C_4H_5 + O_2 reactions indicates that reaction (3) is already at or close to the high-pressure limit (= k_∞) under the current experimental conditions.

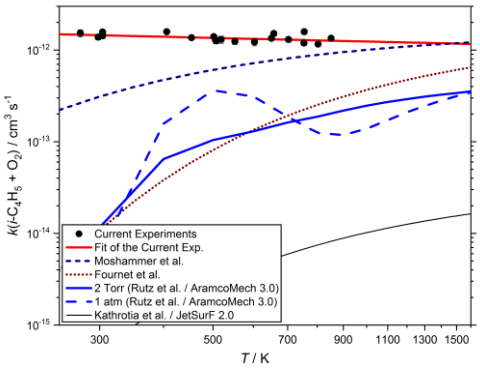

Figure 5. Plot of the current results as well as various predictions for the temperature (and pressure) dependency of the bimolecular rate coefficients for i-C_4H_5 + O_2 → Products reaction.

3.2 Comparison of the current results with literature estimates of i-C_4H_5 + O_2 reaction kinetics

In Figure 5 are shown the bimolecular rate coefficients of *i*-C_4H_5 + O_2 reaction measured in this work as well as fit (F1) that is extrapolated up to 1600 K temperature. Due to the wide temperature range of the experiments, the small scatter of the experimental data, and the very weak negative temperature dependency, current data can be extrapolated to higher temperatures with confidence; it is believed that any significant deviation from the extrapolation is unlikely, even at higher ~1 atm or so pressures. It can be immediately observed that the current results are faster than any prediction, especially at lower temperatures. Indeed, all estimates show clear positive temperature dependency, whereas current experiments show weak negative temperature dependency. What is more, there is a large scatter between kinetic predictions of reaction (3) currently found in literature and combustion models. Scatter is huge around room temperature, but is still more than two orders of magnitude at 1000 K, diminishing to slightly below that at 1500 K. Kathrotia et al.[17] used parameters for reaction (3) in their lower flame temperature ($T \leq 1200$ K) simulations of benzene formation from JetSurf2.0[31], where only one reaction channel, *i*-C_4H_5 + O_2 → H_2CCO + CH_2CHO is included. Clearly, the parameters used in JetSurf2.0 for the *i*-C_4H_5 + O_2 → H_2CCO + CH_2CHO reaction results in significantly smaller values for the bimolecular rate coefficients of reaction (3) over a wide temperature range in comparison to other estimates and especially to the current measurements. Results of master-equation simulations of

reaction (3) performed by Rutz et al.[18] are given in Figure 5 at 2 Torr (corresponding to the current experimental conditions) and at 1 atm pressures. Note that the AramcoMech 3.0[16] model uses the results of Rutz et al., where several reaction channels are open and the kinetics show complicated temperature and pressure-dependencies. The results of Rutz et al. simulations at 2 Torr show positive temperature dependency for reaction (3) and the predicted bimolecular rate coefficient is 25% and 33% of the value predicted by fit (F1) at 1000 and 1500 K, respectively. At 1 atm pressure Rutz et al.[18] simulations show strong positive temperature dependency below about 500 K. However, above about 750 K, Rutz et al. simulations of reaction (3) at 1 atm pressure show slower reactivity than at 2 Torr pressure. In their high-temperature modeling of unsaturated hydrocarbons oxidation, Fournet et al.[32] assumed only the *i*-C_4H_5 + O_2 → CH_2CHCCH + HO_2 channel for reaction (3) (CH_2CHCCH is vinylacetylene) and the estimated bimolecular rate coefficient is shown in Figure 5. According to Figure 1, the rate-limiting transition-state of this channel has an energy that is 12.2 kcal/mol higher than the energy of TS3 and, consequently, might not be an important reaction channel even at high temperatures. The Fournet et al.[32] estimate of the bimolecular rate coefficient of reaction (3) is between 30% and 50% of the value obtained when the current experimental results are extrapolated to 1000 – 1500 K by using expression (F1). Similar to Kathrotia et al.[17] utilizing JetSurf2.0[31] mechanism, Moshammer et al.[5] assumed the *i*-C_4H_5 + O_2 → H_2CCO + CH_2CHO to be the only channel available for reaction (3) in their kinetic model to understand the formation of one- and two-ring aromatic species at 700 Torr pressure in opposed-flow diffusion flames of 1,3-butadiene. However, in this case there is excellent agreement between expression (F1) and the estimate used by Moshammer et al.[5] at 1500 K, see Figure 5.

To determine the kinetics and product distribution of reaction (3) under combustion-relevant conditions, high-level quantum chemical calculations are needed together with a master equation model that accurately accounts for the barrierless R + O_2 addition step(s).[9, 27, 29]

4. Conclusions

Direct, time-resolved kinetic measurements of the *i*-C_4H_5 + O_2 reaction have been performed using photoionization mass spectrometry over wide 275–850 K temperature range at low pressures. The *i*-C_4H_5 radicals were produced principally by 248 nm photolysis of chloroprene. The photolysis of chloroprene also produced 3-methylpropargyl radicals, which have the same mass as *i*-C_4H_5 radicals, but because *i*-C_4H_5 reacts at least 20 times faster with O_2 than 3-methylpropargyl, it was possible to separate the faster *i*-C_4H_5 decay from the slower 3-methylpropargyl decay. The kinetic measurements show that *i*-C_4H_5, a resonantly-stabilized radical, reacts much faster with O_2 than similar-sized propargylic and allylic RSRs. The *i*-C_4H_5 + O_2 reaction possesses weak, negative temperature dependency, not predicted by any estimate or calculation to date. The current work indicates that H_2CO + C_2H_3 + CO and H_2CCO + C_2H_3O are the main product channels. The production of highly reactive vinyl radical (C_2H_3 reacts with O_2 about six times faster than *i*-C_4H_5 at T > 800 K) reduces to some extent the capacity of the *i*-C_4H_5 + O_2 reaction to suppress soot formation.

Acknowledgements

A.J.E., T.T.R, and S.P.J. acknowledge support from the Academy of Finland, Grant Nos. 288377, 311967, and 294042/319353. T.T.P. acknowledges support from the Doctoral Programme in Chemistry and Molecular Sciences of the University of Helsinki.

References

[1] M. Frenklach, Reaction mechanism of soot formation in flames, Phys. Chem. Chem. Phys., 4 (11) (2002) 2028-2037.

[2] S.A. Skeen, H.A. Michelsen, K.R. Wilson, D.M. Popolan, A. Violi, N. Hansen, Near-threshold photoionization mass spectra of combustion-generated high-molecular-weight soot precursors, J. Aerosol. Sci., 58 (2013) 86-102.

[3] N. Hansen, J.A. Miller, T. Kasper, K. Kohse-Höinghaus, P.R. Westmoreland, J. Wang, T.A. Cool, Benzene formation in premixed fuel-rich 1,3-butadiene flames, Proc. Combust. Inst., 32 (2009) 623-630.

[4] K.O. Johansson, M.P. Head-Gordon, P.E. Schrader, K.R. Wilson, H.A. Michelsen, Resonance-stabilized hydrocarbon-radical chain reactions may explain soot inception and growth, Science, 361 (6406) (2018) 997-1000.

[5] K. Moshammer, L. Seidel, Y. Wang, H. Selim, S.M. Sarathy, F. Mauss, N. Hansen, Aromatic ring formation in opposed-flow diffusive 1,3-butadiene flames, Proc. Combust. Inst., 36 (1) (2017) 947-955.

[6] N. Hansen, S.J. Klippenstein, C.A. Taatjes, J.A. Miller, J. Wang, T.A. Cool, B. Yang, R. Yang, L.X. Wei, C.Q. Huang, J. Wang, F. Qi, M.E. Law, P.R. Westmoreland, Identification and chemistry of C_4H_3 and C_4H_5 isomers in fuel-rich flames, J. Phys. Chem. A, 110 (10) (2006) 3670-3678.

[7] D.K. Hahn, S.J. Klippenstein, J.A. Miller, A theoretical analysis of the reaction between propargyl and molecular oxygen, Faraday Discuss., 119 (2001) 79-100.

[8] T.T. Pekkanen, R.S. Timonen, G. Lendvay, M.P. Rissanen, A.J. Eskola, Kinetics and thermochemistry of the reaction of 3-methylpropargyl radical with molecular oxygen, Proc. Comb. Inst., 37 (1) (2019) 299-306.

[9] C.F. Goldsmith, L.B. Harding, Y. Georgievskii, J.A. Miller, S.J. Klippenstein, Temperature and Pressure-Dependent Rate Coefficients for the Reaction of Vinyl Radical with Molecular Oxygen, J. Phys. Chem. A, 119 (28) (2015) 7766-7779.

[10] X. Chen, C.F. Goldsmith, A Theoretical and Computational Analysis of the Methyl-Vinyl + O_2 Reaction and Its Effects on Propene Combustion, J. Phys. Chem. A, 121 (48) (2017) 9173-9184.

[11] S.P. Joshi, T.T. Pekkanen, R.S. Timonen, G. Lendvay, A.J. Eskola, Kinetics of the Methyl-Vinyl Radical + O_2 Reactions Associated with Propene Oxidation, J. Phys. Chem. A, 123 (5) (2019) 999-1006.

[12] M.P. Rissanen, D. Amedro, A.J. Eskola, T. Kurten, R.S. Timonen, Kinetic (T=201-298 K) and Equilibrium (T=320-420 K) Measurements of the C_3H_5 + O_2 reversible arrow $C_3H_5O_2$ Reaction, J. Phys. Chem. A, 116 (16) (2012) 3969-3978.

[13] J. Lee, J.W. Bozzelli, Thermochemical and kinetic analysis of the allyl radical with O_2 reaction system, Proc. Combust. Inst., 30 (2005) 1015-1022.

[14] V.D. Knyazev, I.R. Slagle, Thermochemistry and kinetics of the reaction of 1-methylallyl radicals with molecular oxygen, J. Phys. Chem. A, 102 (45) (1998) 8932-8940.

[15] X.L. Zheng, H.Y. Sun, C.K. Law, Thermochemical and kinetic analyses on oxidation of isobutenyl radical and 2-hydroperoxymethyl-2-propenyl radical, J. Phys. Chem. A, 109 (40) (2005) 9044-9053.

[16] C.W. Zhou, Y. Li, U. Burke, C. Banyon, K.P. Somers, S.T. Ding, S. Khan, J.W. Hargis, T. Sikes, O. Mathieu, E.L. Petersen, M. AlAbbad, A. Farooq, Y.S. Pan, Y.J. Zhang, Z.H. Huang, J. Lopez, Z. Loparo, S.S. Vasu, H.J. Curran, An experimental and chemical kinetic modeling study of 1,3-butadiene combustion: Ignition delay time and laminar flame speed measurements, Combust. Flame, 197 (2018) 423-438.

[17] T. Kathrotia, P. Oßwald, M. Köhler, N. Slavinskaya, U. Riedel, Experimental and mechanistic investigation of benzene formation during atmospheric pressure flow reactor oxidation of *n*-hexane, *n*-nonane, and *n*-dodecane below 1200 K, Combust. Flame, 194 (2018) 426-438.

[18] L.K. Rutz, G. da Silva, J.W. Bozzelli, H. Bockhorn, Reaction of the *i*-C4H5 (CH_2CCHCH_2) Radical with O_2, J. Phys. Chem. A, 115 (6) (2011) 1018-1026.

[19] A.J. Eskola, R.S. Timonen, Kinetics of the reactions of vinyl radicals with molecular oxygen and chlorine at temperatures 200-362 K, Phys. Chem. Chem. Phys., 5 (12) (2003) 2557-2561.
[20] L.N. Krasnoperov, J.T. Niiranen, D. Gutman, C.F. Melius, M.D. Allendorf, Kinetics and Thermochemistry of $Si(CH_3)_3$ + NO Reaction - Direct Determination of a Si-N Bond-Energy, J. Phys. Chem., 99 (39) (1995) 14347-14358.
[21] N. Hansen, S.J. Klippenstein, C.A. Taatjes, J.A. Miller, J. Wang, T.A. Cool, B. Yang, R. Yang, L. Wei, C. Huang, J. Wang, F. Qi, M.E. Law, P.R. Westmoreland, The Identification and Chemistry of C_4H_3 and C_4H_5 Isomers in Fuel-Rich Flames, J. Phys. Chem. A, 110 (2006) 3670-3678.
[22] H.R. Hrodmarsson, J.C. Loison, U. Jacovella, D.M.P. Holland, S. Boye-Peronne, B. Gans, G.A. Garcia, L. Nahon, S.T. Pratt, Valence-Shell Photoionization of C_4H_5: The 2-Butyn-1-yl Radical, J. Phys. Chem. A, 123 (8) (2019) 1521-1528.
[23] W.H. Carothers, Method of Preparing Halobutadienes, U.S. Patent 2,038,538, (1936).
[24] D.E. Szpunar, J.L. Miller, L.J. Butler, F. Qi, 193-nm photodissociation of acryloyl chloride to probe the unimolecular dissociation of CH_2CHCO radicals and CH_2CCO, The Journal of Chemical Physics, 120 (9) (2004) 4223-4230.
[25] J.L. Miller, L.R. McCunn, M.J. Krisch, L.J. Butler, J. Shu, Dissociation of the ground state vinoxy radical and its photolytic precursor chloroacetaldehyde: Electronic nonadiabaticity and the suppression of the H + ketene channel, The Journal of Chemical Physics, 121 (4) (2004) 1830-1838.
[26] E. Delbos, C. Fittschen, H. Hippler, N. Krasteva, M. Olzmann, B. Viskolcz, Rate coefficients and equilibrium constant for the CH_2CHO+O_2 reaction system, J. Phys. Chem. A, 110 (9) (2006) 3238-3245.
[27] A.J. Eskola, T.T. Pekkanen, S.P. Joshi, R.S. Timonen, S.J. Klippenstein, Kinetics of 1-butyl and 2-butyl radical reactions with molecular oxygen: Experiment and theory, Proc. Combust. Inst., 37 (1) (2019) 291-298.
[28] M. Döntgen, T.T. Pekkanen, S.P. Joshi, R.S. Timonen, A.J. Eskola, Oxidation Kinetics and Thermodynamics of Resonance-Stabilized Radicals: The Pent-1-en-3-yl + O_2 Reaction, The Journal of Physical Chemistry A, 123 (37) (2019) 7897-7910.
[29] C.P. Moradi, A.M. Morrison, S.J. Klippenstein, C.F. Goldsmith, G.E. Douberly, Propargyl + O_2 Reaction in Helium Droplets: Entrance Channel Barrier or Not?, J. Phys. Chem. A, 117 (50) (2013) 13626-13635.
[30] V.D. Knyazev, I.R. Slagle, Kinetics of the Reaction of Vinyl Radical with Molecular Oxygen, J. Phys. Chem., 99 (8) (1995) 2247-2249.
[31] H. Wang, B. Sirjean, D. A. Sheen, R. Tango, A. Violi, J. Y. W. Lai, F. N. Egolfopoulos, D. F. Davidson, R. K. Hanson, C. T. Bowman, C. K. Law, W. Tsang, N. P. Cernansky, D. L. Miller, R. P. Lindstedt, http://web.stanford.edu/group/haiwanglab/JetSurF/JetSurF2.0/index.html
[32] R. Fournet, J.C. Bauge, F. Battin-Leclerc, Experimental and modeling of oxidation of acetylene, propyne, allene and 1,3-butadiene, Int. J. Chem. Kinet., 31 (5) (1999) 361-379.

Separate List of Figure Captions

Scheme 1. Two resonance (Kekulé) structures of *i*-C_4H_5 radical. Left: vinylic structure, Right: allenic structure.

Figure 1. Enthalpy profile of *i*-C_4H_5 + O_2 reaction according to Rutz[18] et al. with G3SX enthalpies. See text on discussion of transition-state 1(**TS1**) and **TS2** energies.

Figure 2. Plot of the first order *i*-C_4H_5 and 3-methylpropargyl decay rate coefficients k_3' and k_4' *versus* [O_2] at T = 852 K and 2.83 Torr pressure (see table S1). Insets show actual ion signal profiles for the combined *i*-C_4H_5 and 3-methylpropargyl decays in the absence of the O_2-reactant (right) and in the presence of the [O_2] = 1.9×10^{14} cm^{-3} (left). Values of k_{3wall}' shown as solid black square and solid red triangle at [O_2] = 0 in the plot were measured at first and the end of experiments and k_{4wall}' in the fits was fixed to the value obtained from extrapolating k_4' values to [O_2] = 0. Uncertainties are one-standard deviation (1σ).

Figure 3. Plots of *i*-C_4H_5 and 3-methylpropargyl radical decay with fit results (k_3' and k_4') and observed formations and fits of ketene and formaldehyde as products of *i*-C_4H_5 + O_2 reaction. Chloroprene was photolytic precursor and uncertainties shown are one-standard deviation (1σ). Ketene and formaldehyde formation kinetics agree within 2σ-uncertainty with *i*-C_4H_5 decay rate.

Figure 4. Plot of bimolecular rate coefficients of *i*-C_4H_5 reaction measured in this work versus temperature. Also shown are the obtained fit to the data and 95 % confidence limits.

Figure 5: Plot of the current results as well as various predictions for the temperature (and pressure) dependency of the bimolecular rate coefficients for *i*-C_4H_5 + O_2 → Products reaction.

Supplemental Material (SM), content, and list of captions

File name: SM for First Direct Kinetic Measurement of *i*-C_4H_5 (CH_2CHCCH_2) + O_2 Reaction: Toward Quantitative Understanding of Aromatic Ring Formation Chemistry (Proc. Combust. Inst. 38, 2021).docx; Contains (1) The chemical structures of benzene, fulvene and phenyl radical (2) Energetics of chloroprene photolysis at 248 nm (3) A comparison of kinetics of *i*-C_4H_5 + O_2 and CH_2CCCH_3 + O_2 reactions (4) The chloroprene (2-chloro-1,3-butadiene) synthesis (5) Experimental product study of chloroprene 248 nm photolysis (6) The table of conditions and measured bimolecular reaction rate coefficients in this work.

Scheme S1. The chemical structures of benzene, fulvene and phenyl radical.

Figure S1. A reaction enthalpy profile at zero kelvin displaying the possible photolysis products of chloroprene at 248 nm. Important C_4H_5 isomers for this work are inside the red ellipse. It can be seen that at 248 nm photolysis CH_2CHCCH_2 (*i*-C_4H_5) and CH_2CCCH_3 (3-methylpropargyl) radicals can be formed but not $CH_2CHCHCH$ (*n*-C_4H_5). Accuracy of the calculations is expected to be good enough to rule out *n*-C_4H_5 formation.

Figure S2. A comparison of bimolecular rate coefficients of *i*-C_4H_5 + O_2 (this work) and CH_2CCCH_3 + O_2 (3-methylpropargyl + O_2, previous work) reactions versus temperature.

Table S1. Conditions and results of the experiments used to measure the bimolecular rate coefficients of *i*-C_4H_5 + O_2 reaction. The shown error limits in k_w and k_{exp} are 1σ fitting uncertainties only.